Structural and Mechanical Properties of Zr-Si-N Thin Films Prepared by Reactive Magnetron Sputtering

Flávio Gustavo Ribeiro Freitas[a]*, Roberto Hübler[b], Gabriel Soares[c],

Amanda Gardênia Santos Conceição[a], Edson Reis Vitória[a], Renata Gomes Carvalho[a],

Eduardo Kirinus Tentardini[a]

[a]*Departamento de Ciência e Engenharia de Materiais, Universidade Federal de Sergipe – UFS,
Avenida Marechal Rondon, s/n, CEP 49100-000, São Cristóvão, SE, Brazil*
[b]*Instituto de Física – GEPSI, Pontifícia Universidade Católica do Rio Grande do Sul – PUCRS,
Avenida Ipiranga, 6681, CEP 90619-900, Porto Alegre, RS, Brazil*
[c]*Instituto de Física, Universidade Federal do Rio Grande do Sul – UFRGS,
Avenida Paulo Gama, 110, CEP 90040-060, Porto Alegre, RS, Brazil*

Zirconium silicon nitride (ZrSiN) thin films were deposited by reactive magnetron sputtering in order to verify the silicon influence on coating morphology and mechanical properties. The Si/(Zr+Si) ratio was adjusted between 0 to 15% just modifying the power applied on the silicon target. Only peaks associated to ZrN crystalline structure were observed in XRD analysis, since Si_3N_4 phase was amorphous. All samples have (111) preferred orientation, but there is a peak intensity reduction and a broadening increase for the sample with the highest Si/(Zr+Si) ratio (15%), demonstrating a considerable loss of crystallinity or grain size reduction (about 8 nm calculated by Scherrer). It was also observed that the I(200)/I(111) ratio increases with silicon addition. Chemical composition and thickness of the coatings were determined by RBS analysis. No significant changes in nanohardness with increasing Si content were found. The morphology observed by FEG-SEM presents non columnar characteristics for thin films with silicon addition. The set of results suggests that Si addition is restricting the columnar growth of ZrN thin films. This conclusion is justified by the fact that Si contributes to increase the ZrN grains nucleation during the sputtering process.

Keywords: *thin films, ZrSiN, magnetron sputtering, nanohardness, RBS*

1. Introduction

Nitride transition metal thin films have been used in the last decades due to properties as hardness and wear resistance[1-3]. Zirconium nitride (ZrN) is a typical coating used because its tribological properties, besides corrosion and oxidation resistance. Even with differentiated properties, ZrN thin films present columnar microstructure, micro-cracks and pores, which are defects associated with transition metals nitrides deposited by PVD and CVD techniques. These coatings characteristics allow direct contact between the external environment and the substrate, compromising the mechanical properties and its applications in high temperature or corrosive environments[4-6].

It is important to note that ZrN thin films mechanical properties are associated with a complex state of compression of the crystalline lattice (residual stress). The deposition process is usually carried out at low temperatures (T < 300 °C) inhibiting ZrN molecules to achieve its equilibrium state in the lattice structure. The result is that the crystalline lattice remains in a metastable condition and, consequently, the structure can be changed if the necessary activation energy is

provided to the system, resulting in degradation of coatings properties[7-9].

An alternative to modify ZrN thin films microstructure and morphology is the addition of a third element as silicon. The Si addition promotes a two phase microstructure formation: a crystalline (ZrN) and an amorphous phase (Si_3N_4). The amorphous phase is located at the grain boundaries and contributes to reduce the ZrN grain size, since it increases the ZrN grains nucleation rate. The final grain size is less than 10 nm, resulting in the formation of a nanocomposite structure. These characteristics have potential to change thin film morphology and macroscopic properties[10-12].

This type of microstructure is dense, homogeneous and not significantly affected by diffusion activated processes, which means that it has a high thermal stability[13-17]. But, properties and microstructure of ZrSiN thin films are function of silicon concentration and deposition techniques (PVD or CVD) parameters. So, although many studies demonstrate the advantages of adding silicon to nitride thin films, there are gaps and discussions about microstructure formation and influence of Si content and deposition parameters on coatings physical and chemical properties[2,3,7-17].

*e-mail: flaviogus@hotmail.com

The study proposal was to deposit thin films of ZrSiN system by reactive magnetron sputtering (RMS) varying the Si concentration in each coating. Grazing Angle X-ray diffraction (GAXRD), Field Emission Scanning Electron Microscopy (FEG-SEM), Rutherford Backscattering Spectroscopy (RBS) and nanohardness techniques were used to analyze coatings morphology and mechanical properties.

2. Material and Methods

Thin films used in this work were co-deposited by reactive magnetron sputtering with an AJA Orion 5-HV Sputtering Systems model with two independents targets, Zr and Si, with purity of 99.7 at% and 99.5 at %, respectively. Before deposition, substrates were underwent ultrasonic cleaning in acetone during 30 minutes, washed with ethyl alcohol (54°) and then dried. The chamber was preconditioned to a base pressure of 1×10^{-7} Torr and targets were bombarded ionically to remove oxide layers from the surface before deposition.

All deposition parameters were maintained constant during depositions except the power used at silicon target, as showed in Table 1. The distance target-substrate applied in all depositions was 120 mm and two different types of substrates were used according to the characterization technique: silicon wafer for GAXRD, nanohardness and FEG-SEM analysis and polyethylene plates for RBS studies. The thickness and deposition time was also adjusted to comply with the required analysis, 50 nm and 12 minutes for RBS samples, 300 nm and 60 minutes for FEG-SEM and GAXRD samples and 600 nm and 120 minutes for nanohardness samples. No external heating was applied to the substrates.

GAXRD patterns were performed on a Shimadzu XRD-6000 model (Cu-Kα radiation; λ = 1.54 Å) with grazing angle of 1°. The morphology of the film cross section was observed on a high-resolution FEG-SEM JSM-6330F.

Nanohardness analyses were performed in a Fisherscope HV 100 with a Berkovich indenter and indentation depth of 40 nm. This technique also permits to determine the films Young's modulus. RBS analysis were performed using a 3 MV tandetron with alpha particles accelerated up to 2 MeV, with a silicon based detector at an angle of 165° and resolution of 12 keV.

3. Results and Discussion

Stoichiometric zirconium nitride thin films has a metallic gold color[18] and the ZrN coating deposited in this work with Ar/N₂ ratio of 19/2 presented this characteristic. A set of ZrSiN thin films modifying Si concentration were deposited using different powers applied on the silicon target. These samples were analyzed by RBS technique to measure coatings

thickness, identify chemical elements and their respective concentrations. All samples present similar results, except the silicon peak, which is function of the power applied to the Si target. For this reason it is presented in Figure 1 just the RBS analysis for sample ZrSiN_3.

Analyzing Figure 1 is possible to identify the presence of Hf, Zr, Si, N and O from thin film and C from substrate and these chemical elements were detected for all samples. The hafnium presence is due the contamination of this chemical element on Zr target, once by manufacturer data the target is 99.7% Zr and 0.3% Hf. RBS results also show that the films are near the stoichiometric concentration, confirming the Ar/N₂ ratio of 19/2. The areal densities of zirconium and nitrogen chemical species were determined using a Sb implanted silicon standard.

Table 2 shows Zr, N and Si concentration in at.% and Si/(Zr+Si) ratio determined by RBS for all samples. The coatings Si/(Zr+Si) ratio were characterized as low (6.2 %), intermediary (8.0 %) and high (15.0 %), for sample ZrSiN_1, ZrSiN_2 and ZrSiN_3, respectively. The coatings thickness was estimated in approximately 60 nm for all samples.

Figure 2 shows the GAXRD analysis for all samples. The ZrN, ZrSiN_1 and ZrSiN_2 XRD patterns are almost identical, but the ZrSiN_3 has a peak intensity reduction and a small increase in (111) peak width, demonstrating a considerable loss of crystallinity or grain size reduction. Si_3N_4 structure is amorphous (confirmed by GAXRD analysis) and its presence causes the reduction of diffraction peaks intensity. Si_3N_4 particles contribute to ZrN grain nucleation process during film growth, resulting in a structure with reduced grain size[10,19]. The crystallite size calculated by Scherrer for ZrSiN_3 is about 8 nm (nanocomposite structure), while
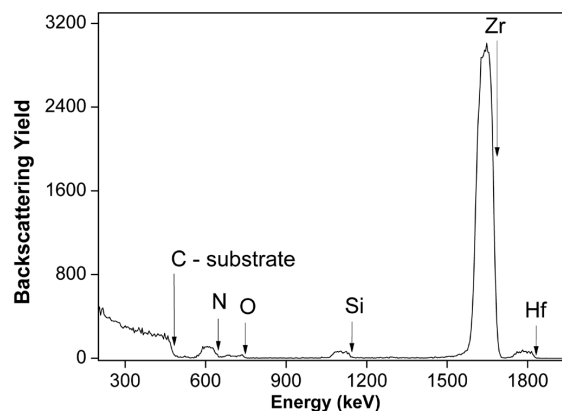

Figure 1. RBS analysis for sample ZrSiN_3. Coatings compositions are almost stoichiometric.

Table 1. Sputtering deposition parameters – only power applied to silicon target was changed in thin films samples.

Sample	Working Pressure [mTorr]	Zr DC Power [W/cm²]	Si RF Power [W/cm²]	Ar flux [sccm]	N₂ flux [sccm]
ZrN	3.0	6.0	0.0	19.0	2.0
ZrSiN_1	3.0	6.0	1.2	19.0	2.0
ZrSiN_2	3.0	6.0	2.2	19.0	2.0
ZrSiN_3	3.0	6.0	3.7	19.0	2.0

for others films is 11 nm. A small peak at 54° was found for all samples and is probably associated with ZrO_2 or $ZrSiO_4$ phases.

Reference pattern ICDD PDF 35-0753 presented in Figure 2 shows that the main peaks for ZrN are (111) and (200) orientations, with this last presenting an intensity of 70% compared with (111) peak. Comparing the ICDD pattern with the ZrN and ZrSiN coatings deposited on this work, it is clear the decreasing of (200) peak intensity, showing that there is a high fraction of (111) oriented grains when compared to others orientations, especially the (200) grains. It is important to note that as the silicon content is increased, it can be observed that I(200)/I(111) ratio is increased from 14.2% to 18.9%, showing that (200) grains growth during deposition is favored due the silicon content. These results can be better observed in Figure 3.

Grains with (200) orientation have the lowest surface energy, while (111) grains have the lowest deformation energy. Thin films deposited by sputtering have high defects concentration, which causes crystal lattice distortion and promotes the (111) preferred orientation due to deformation energy minimization[20,21]. Grains with (111) orientation grow in the normal direction to the film plane, which contributes to the formation of a columnar microstructure, while (200) grains grow in the parallel direction, having the potential to change the columnar morphology to a non columnar one[22].

The silicon addition act as a nucleation center for ZrN grains, reducing the crystallite size and creating thermodynamic conditions to the (200) oriented grains. The (200) indicates that the system is minimizing the surface energy and it can be concluded that the amount of defects in the film is reduced, which can improve thin film properties and characteristics.

Figure 4 shows nanohardness results for ZrN and ZrSiN thin films. The ZrN hardness was determined in about 15.6 GPa, value consistent with literature. Samples ZrSiN_1, ZrSiN_2 and ZrSiN_3 had no significant variation in nanohardness. For ZrSiN_1 and ZrSiN_2 the Si addition in low concentration was not enough to change the structure and mechanical properties. But, for ZrSiN_3 the highest I(200)/I(111) ratio contributes to hardness reduction and, on the other hand, the lowest crystallite size and the microstructure composed by ZrN and Si_3N_4 phases contributes to increase this mechanichal propertie[23]. The global result is no significant impact in hardness for ZrSiN_3 sample.

Young's modulus results (Figure 4) has similar trend as observed for hardness values and the same interpretations can be pointed out for this mechanichal propertie.

Figure 5 shows FEG-SEM of ZrSiN_2 thin film cross section with a non columnar structure. All ZrSiN coatings presented this same behavior. Silicon addition promoted a transition from a columnar morphology to a non columnar one as the Si content is increased. This microstructure is aligned
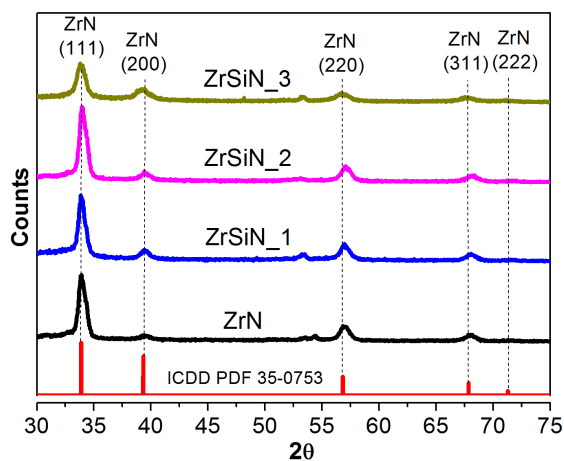

Figure 2. Grazing angle (1°) XRD analysis – (111) peak intensity reduction and broadening for ZrSiN_3 sample. It can be verified the (111) preferred orientation for ZrN and ZrSiN thin films. The peaks intensities obtained from ICDD PDF 35-0753 are also presented.
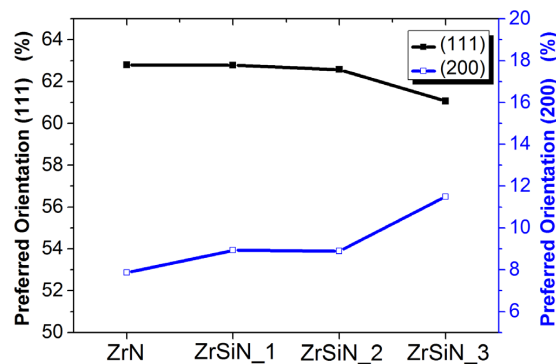

Figure 3. Preferred orientation obtained from GAXRD 1° – I(200)/I(111) ratio is higher as Si content is increased.
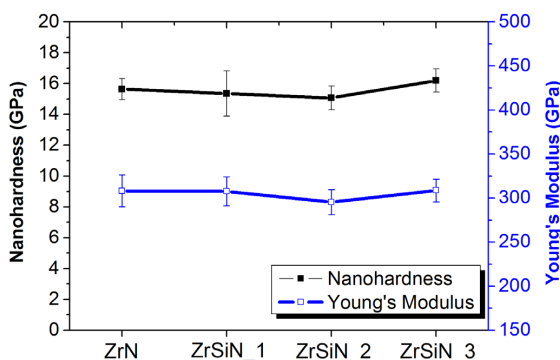

Figure 4. Nanohardness and Young's Modulus – it is verified no significant changes for all films deposited.

Table 2. RBS analysis to N, Zr and Si – chemichal concentrations and thin film thickness.

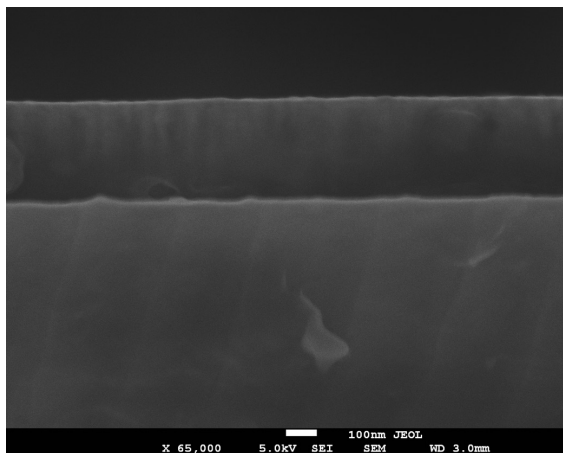| Sample	N [at. %]	Zr [at. %]	Si [at. %]	Si / (Zr+Si) [%]	Thickness [nm]
ZrN	48.5±0.6	51.5±0.6	-	-	57±9
ZrSiN_1	48.4±0.6	48.4±0.6	3.2±0.1	6.2±0.3	59±10
ZrSiN_2	49.4±0.7	46.5±0.7	4.1±0.1	8.0±0.2	58±10
ZrSiN_3	48.9±0.8	43.5±0.8	7.6±0.1	15.0±0.2	68±9

Figure 5. FEG-SEM image for ZrSiN_2 – it can be observed a morphology composed by non columnar structure.

with GAXRD results, confirming the Si potential to modify ZrN morphology by blocking the columnar structure growth. In other words, silicon atoms restricts the columnar growth due to an increase in ZrN grain nucleation rate, inhibiting the (111) orientation and favoring the (200) orientation.

It can be also verified that the thin films observed by FEG-SEM are homogeneous and have apparently good adhesion.

4. Conclusions

ZrN and ZrSiN were successively deposited by reactive magnetron sputtering. RBS analysis show ZrN coatings with stoichiometric near to 1:1 and the Si/(Zr+Si) ratio of ZrSiN

coatings were determined as 6.2%, 8.0% and 15.0% when applied 1.2, 2.2 and 3.7 W/cm² at Si target, respectively. All coatings presented hafnium originated from zirconium target.

GAXRD patterns show a (111) peak broadening and intensity reduction for sample ZrSiN _3, but maintaining the preferred orientation (111). The crystallite size calculated by Scherrer pointed out that silicon addition creates a nanocomposite structure.

All thin films present a high fraction of (111) oriented grains, however it is observed an increase in I(200)/I(111) ratio in function of silicon content. Silicon addition creates thermodynamic conditions to deposit (200) oriented grains, which causes a reduction in films defects concentration.

Nanohardness analysis indicated no significant modification in hardness between ZrN and ZrSiN coatings. But, ZrSiN_3 sample has a set of characteristics that justifies the maintainability of its nanohardness (I(200)/I(111) ratio increase, crystallite size reduction and microstructure composed by two phases). Young's modulus have the same behaviour observed for nanohardness analyses.

FEG-SEM results show ZrSiN thin films with a non columnar structure. Silicon addition blocks the columnar growth due to the favorable conditions to (200) orientation. Increasing the Si content in ZrN thin films promotes a transition from a columnar to a non columnar structure.

Acknowledgements

References

1. Musil J. Hard and superhard nanocomposite coatings. *Surface and Coatings Technology*. 2000; 125(1-3):322-330. http://dx.doi.org/10.1016/S0257-8972(99)00586-1.

2. Benkahoul M, Sandu CS, Tabet N, Parlinska-Wojtan M, Karimi A and Lévy F. Effect of Si incorporation on the properties of niobium nitride films deposited by DC reactive magnetron sputtering. *Surface and Coatings Technology*. 2004; 188-189:435-439. http://dx.doi.org/10.1016/j.surfcoat.2004.08.048.

3. Veprek S and Veprek-Heijman MGJ. Industrial applications of superhard nanocomposite coatings. *Surface and Coatings Technology*. 2008; 202(21):5063-5073. http://dx.doi.org/10.1016/j.surfcoat.2008.05.038.

4. Abadias G, Michel A, Tromas C, Jaouen C and Dub SN. Stress, interfacial effects and mechanical properties of nanoscale multilayered coatings. *Surface and Coatings Technology*. 2007; 202(4-7):844-853. http://dx.doi.org/10.1016/j.surfcoat.2007.05.068.

5. Lee J and Yang G. Preparation of TiAlN/ZrN and TiCrN/ZrN multilayers by RF magnetron sputtering. *Transactions of Nonferrous Metals Society of China.* 2009; 19(4):795-799. http://dx.doi.org/10.1016/S1003-6326(08)60352-0.

6. Ma S, Prochazka J, Karvankova P, Ma Q, Niu X, Wang X, et al. Comparative study of the tribological behavior of superhard nanocomposite coatings nc-TiN/a-Si3N4 with TiN. *Surface and Coatings Technology*. 2005; 194(1):143-148. http://dx.doi.org/10.1016/j.surfcoat.2004.05.007.

7. Veprek S, Veprek-Heijman MGJ, Karvankova P and Prochazka J. Different approaches to superhard coatings and nanocomposites. *Thin Solid Films*. 2005; 476(1):1-29. http://dx.doi.org/10.1016/j.tsf.2004.10.053.

8. Veprek S and Veprek-Heijman MGJ. Limits to the preparation of superhard nanocomposites: impurities, deposition and annealing temperature. *Thin Solid Films*. 2012; 522:274-282. http://dx.doi.org/10.1016/j.tsf.2012.08.048.

9. Veprek S, Mannling HD, Karvánková P and Procházka J. The issue of the reproducibility of deposition of superhard nanocomposites with hardness of ≥50 GPa. *Surface and Coatings Technology*. 2006; 200(12-13):3876-3885. http://dx.doi.org/10.1016/j.surfcoat.2004.11.023.

10. Sandu CS, Sanjinés R and Medjani F. Control of morphology (ZrN crystallite size and SiNx layer thickness) in Zr–Si–N nanocomposite thin films. *Surface and Coatings Technology*. 2008; 202(11):2278-2281. http://dx.doi.org/10.1016/j.surfcoat.2007.09.003.

11. Pilloud D, Pierson JF and Takadoum J. Structure and tribological properties of reactively Zr-Si-N films. *Thin Solid Films*. 2006; 496(2):445-449. http://dx.doi.org/10.1016/j.tsf.2005.09.062.

12. Sandu CS, Harada S, Sanjinés R and Cavaleiro A. A unique approach to reveal the nanocomposite nc-MN/SiN-layer architecture of thin films via electrical measurements. *Surface and Coatings Technology*. 2010; 204(12-13):1907-1913. http://dx.doi.org/10.1016/j.surfcoat.2009.11.045.

13. Sandu CS, Sanjinés R, Benkahoul M, Medjani M and Lévy F. Formation of composite ternary thin films by magnetron sputtering co-deposition. *Surface and Coatings Technology*. 2006; 201(7):4083-4089. http://dx.doi.org/10.1016/j.surfcoat.2006.08.100.

14. Sandu CS, Medjani F, Sanjinés R, Karimi A and Lévy F. Structure, morphology and electrical properties of sputtered Zr–Si–N thin films: from solid solution to nanocomposite. *Surface and Coatings Technology*. 2006; 201(7):4219-4223. http://dx.doi.org/10.1016/j.surfcoat.2006.08.002.

15. Sandu CS, Benkahoul M, Sanjinés R and Lévy F. Model for the evolution of Nb–Si–N thin films as a function of Si content relating the nanostructure to electrical and mechanical properties. *Surface and Coatings Technology*. 2006; 201(6):2897-2903. http://dx.doi.org/10.1016/j.surfcoat.2006.06.003.

16. Sandu CS, Cusnir N, Oezer D, Sanjinés R and Patscheider J. Influence of bias voltage on the microstructure and physical properties of magnetron sputtered Zr–Si–N nanocomposite thin films. *Surface and Coatings Technology*. 2009; 204(6-7):969-972. http://dx.doi.org/10.1016/j.surfcoat.2009.06.042.

17. Patscheider J, Zehnder T and Diserens M. Structure–performance relations in nanocomposite coatings. *Surface and Coatings Technology*. 2001; 146-147:201-208. http://dx.doi.org/10.1016/S0257-8972(01)01389-5.

18. Lamni R, Martinez E, Springer SG, Sanjines R, Schmid PE and Levy F. Optical and electronic properties of magnetron sputtered ZrNx thin films. *Thin Solid Films*. 2004; 447-448:316-321. http://dx.doi.org/10.1016/S0040-6090(03)01109-X.

19. Musil J. Hard nanocomposite coatings: thermal stability, oxidation resistance and toughness. *Surface and Coatings Technology*. 2012; 207:50-65. http://dx.doi.org/10.1016/j.surfcoat.2012.05.073.

20. Abadias G. Stress and preferred orientation in nitride-based PVD coatings. *Surface and Coatings Technology*. 2008; 202(11):2223-2235. http://dx.doi.org/10.1016/j.surfcoat.2007.08.029.

21. Goldfarb I, Pelleg J, Zevin L and Croitoru N. Lattice distortion in thin films of IVB metal (Ti, Zr, Hf) Nitrides. *Thin Solid Films*. 1991; 200(1):117-127. http://dx.doi.org/10.1016/0040-6090(91)90034-U.

22. Banerjee R, Chandra R and Ayyub P. Influence of the sputtering gas on the preferred orientation of nanocrystalline titanium nitride thin films. *Thin Solid Films*. 2002; 405(1-2):64-72. http://dx.doi.org/10.1016/S0040-6090(01)01705-9.

23. Procházka J, Karvánková P, Veprek-Heijman MGJ and Veprek S. Conditions required for achieving superhardness of ≥ 45 GPa in nc-TiN/a-Si3N4 nanocomposites. *Materials Science and Engineering A*. 2004; 384(1-2):102-116. http://dx.doi.org/10.1016/j.msea.2004.05.046.